Published in final edited form as:
Nat Neurosci. 2014 July ; 17(7): 908–910. doi:10.1038/nn.3725.

Leptin signaling in GFAP-expressing adult glia cells regulates hypothalamic neuronal circuits and feeding

Jae Geun Kim1, **Shigetomo Suyama**[1], **Marco Koch**[1,5], **Sungho Jin**[1], **Pilar Argente-Arizon**[6], **Jesus Argente**[6], **Zhong-Wu Liu**[1], **Marcelo R. Zimmer**[1], **Jin Kwon Jeong**[1,2], **Klara Szigeti-Buck**[1], **Yuanqing Gao**[7], **Cristina Garcia-Caceres**[7], **Chun-Xia Yi**[7], **Natalina Salmaso**[3], **Flora M. Vaccarino**[3,4], **Julie Chowen**[6], **Sabrina Diano**[1,2,4], **Marcelo O Dietrich**[1], **Matthias H. Tschöp**[7], and **Tamas L. Horvath**[1,2,4]

[1]Program in Integrative Cell Signaling and Neurobiology of Metabolism, Section of Comparative Medicine, Yale University School of Medicine, New Haven CT 06520, USA

[2]Department of Obstetrics, Gynecology, and Reproductive Sciences, Yale University School of Medicine, New Haven CT 06520, USA

[3]Child Study Center, Yale University School of Medicine, New Haven CT 06520, USA

[4]Department of Neurobiology, Yale University School of Medicine, New Haven, CT 06520, USA

[5]Institute of Anatomy, University of Leipzig, 04103 Leipzig, Germany

[6]Hospital Infantil Universitario Niño Jesús, Department of Endocrinology, Instituto de Investigación La Princesa and Centro de Investigación Biomédica en Red de la Fistiopatología (CIBER) de Fisiopatología de Obesidad y Nutrición, Instituto de Salud Carlos III, Madrid, Spain

[7]Institute for Diabetes and Obesity, Helmholtz Zentrum München & Technische Universität München, Germany

Abstract

We have shown that synaptic re-organization of hypothalamic feeding circuits in response to metabolic shifts involves astrocytes, cells that can directly respond to the metabolic hormone, leptin, *in vitro*. It is not known whether the role of glia cells in hypothalamic synaptic adaptions is active or passive. Here we show that leptin receptors are expressed in hypothalamic astrocytes and that conditional, adult deletion of leptin receptors in astrocytes leads to altered glial morphology, decreased glial coverage and elevated synaptic inputs onto pro-opiomelanocortin (POMC)- and Agouti-related protein (AgRP)-producing neurons. Leptin-induced suppression of feeding was diminished, while rebound feeding after fasting or ghrelin administration was elevated in mice with astrocyte-specific leptin receptor deficiency. These data unmask an active role of glial cells in the initiation of hypothalamic synaptic plasticity and neuroendocrine control of feeding by leptin.

Contributions: J.G.K., M.O.D. and T.L.H. designed the study. J.G.K., M.H.T. and T.L.H. interpreted the results. J.G.K. and S.J. performed experiments and analyzed the data. M.K. and K.S.B. contributed to Figure 1h-j and 2a-c. J.K.J. and S.D. contributed to Figure 1c. S.S. and Z.L. contributed to Figure 2 d-g and Supplementary Figure 6. M.R.Z., N.S. and F.M.V. contributed to Supplementary Figure 1 and 4a. P.A., J.C. and J.A. contributed to Supplementary Figure 3b. Y.G., C.G. and C.Y. contributed to the generation of animal model. J.G.K and T.L.H. wrote the paper with input from the other authors.

Astrocytes are the most abundant cells in the central nervous system (CNS), yet at times, they have been relegated a less than prominent role in the control of complex brain functions supported by neuronal circuits[1,2]. The regulation of food intake and energy expenditure is tightly linked to synaptic plasticity of hypothalamic neural circuits[3,4], processes in which glial cells have also been implicated[5,6]. It has not yet been explored whether this involvement of glia is secondary or plays an active role in the promotion of these processes initiated by leptin[7].

As previously reported, the long form of leptin receptors (*LepR*) was found to be located in astrocytes through the use of immunocytochemistry[8,9]. However, due to questions regarding antibody specificity, it still remains controversial whether astrocytes express functional *LepR*. We found immunolabeling of glial fibrillary acidic protein (GFAP) in a subset of leptin receptor (*LepR*)-driven EGFP-expressing cells (Fig. 1a). Second, *LepR* mRNA was detected from translating ribosomes of astrocytes (Supplementary Fig. 1). Third, mRNA of *LepR* was expressed in purified mouse hypothalamic astrocytes using astrocyte primary culture (Supplementary Fig. 3b).

To test the role of the long form of leptin receptors in glial cells, we generated a genetic mouse model in which leptin receptors are time-specifically ablated in astrocytes. Because glial cells are the progenitor cells for neurogenesis during brain development[10], we used a tamoxifen-inducible *Cre-ERT2* system to allow cell and time-specific knockout of leptin receptor in adult astrocytes (Supplementary Fig. 3a). To assess whether functional Cre protein was restricted to astrocytes and induced by tamoxifen injection, we crossed GFAP-CreERT2 mice with tdTomato-loxP reporter mice, which express red fluorescent protein. We confirmed successful Cre-mediated recombination in GFAP-positive cells by detecting tdTomato-positive cells after injection of tamoxifen (Supplementary Fig. 2c). This recombination was found to be specific to astrocytes as the tdTomato-positive cells did not express Iba-1 (a marker for microglia) or NeuN (a marker for neurons) (Supplementary Fig. 2c). In addition, we combined *in situ* hybridization (ISH) with immunohistochemistry (IHC) to validate the selective loss of functional leptin receptors from GFAP-positive cells in mice that are GFAP-Cre transgenic and homozygous for the loxP-modified leptin receptor allele (Fig. 1b,c). We further confirmed the deletion of leptin receptor exon 17 in astrocyte primary cells of GFAP-LepR$^{-/-}$ mice by reverse transcriptase (RT)-polymerase chain reaction (PCR) (Supplementary Fig. 3b).

Because of our previous findings that leptin affects glial morphology,[6,11] we first analyzed astrocytes in the arcuate nucleus of mice following leptin receptor knockout. Astrocyte-specific loss of leptin receptors did not alter the total number of GFAP-positive cells in the hypothalamus (Fig. 1e). However, GFAP-LepR$^{-/-}$ mice showed fewer numbers (Fig. 1f) and shorter lengths (Fig. 1g) of primary astrocytic projections. We also analyzed astrocytes in the hippocampus. Interestingly, we could detect *LepR* mRNA in the hippocampus (Supplementary Fig. 4a), but there were no significant changes regarding number and morphology of GFAP-positive cells (Supplementary Fig. 4b–e).

Previously, we reported that astrocytic processes are involved in synaptic plasticity of feeding circuits, including those comprising the proopiomelanocortin (POMC) neurons that

secrete α-melanocyte stimulating hormone (α-MSH) and AgRP (agouti-related protein) neurons that coproduce neuropeptide Y (NPY) and γ-amino-butyric acid (GABA)[5, 6]. This led us to evaluate the patterns of glial ensheathment onto the perikaryal membranes of POMC and unlabeled neurons in the arcuate nucleus by electron microscopy (EM). GFAP-LepR$^{-/-}$ mice had lower glial coverage on the perikaryal membranes of POMC (Fig. 1i) and unlabeled neurons (Fig. 1j) compared to that of control mice. We then analyzed glial coverage of POMC and AgRP cells of GFAP-LepR$^{-/-}$ mice through the use of double immunofluorescence: GFAP immonolabeled with red fluorescence in association with green fluorescent protein (GFP)-labeled POMC or AgRP neurons (*Npy-hrGFP* mice were used for the latter; these mice allow visualization of AgRP neurons due to the co-expression of NPY and AgRP in these cells). We found that direct contacts were lower between astrocytes and either POMC (Supplementary Fig. 5a,b) or AgRP (Supplementary Fig. 5c,d) neurons in GFAP-LepR$^{-/-}$ mice relative to control values.

Next, we assessed whether reduced astrocyte coverage affects synapse number on arcuate nucleus neurons. First, we analyzed synapse number and type by EM. We found that there were elevated numbers of both symmetric and asymmetric synapses on both POMC (Fig. 2b) and unlabeled neuronal perikarya (Fig. 2c) in GFAP-LepR$^{-/-}$ mice relative to controls. To corroborate these anatomical findings, miniature postsynaptic currents (mPSCs) onto POMC and AgRP neurons were analyzed. We found an elevated frequency of miniature inhibitory postsynaptic currents (mIPSCs) (Fig. 2d) but no change in frequency of miniature excitatory postsynaptic currents (mEPSCs) onto POMC cells (Fig. 2e). AgRP neurons had an increase in the frequency of both mIPSCs and mEPSCs (Fig. 2f,g). Taken together, these data show that leptin receptor signaling in astrocytes regulates the synaptic input organization of AgRP and POMC cells. We also revealed an increased amplitude of both mIPSCs and mEPSCs onto the POMC neurons of GFAP-LepR$^{-/-}$ mice (Supplementary Fig. 6c,d). On the other hand, there was no alteration in the amplitude of mPSCs onto the AgRP neurons (Supplementary Fig. 6a,b). These findings suggest that the reduced astrocyte coverage may affect the signaling pathways linked to the postsynaptic receptors of POMC neurons presumably by buffering trophic factors in the respective synaptic cleft area.

We have shown that the synaptic input organization of the melanocortin system predicts behavioral output of the melanocortin system in the face of a changing metabolic milieu[3, 5, 12]. Thus, we next assessed the metabolic phenotype, including body weight, body composition, food intake and energy expenditure, of GFAP-LepR$^{-/-}$ mice and their littermate controls. Three-month-old GFAP-LepR$^{-/-}$ mice showed no differences in metabolic phenotypes under standard feeding conditions (Supplementary Fig. 7a–h). However, the effect of both single and multiple injections of leptin to suppress feeding were diminished in GFAP-LepR$^{-/-}$ mice relative to controls (Fig. 3a,b). Consistent with these results, leptin-stimulated Fos activity was attenuated in the GFAP-LepR$^{-/-}$ mice (Fig. 3c,d). These findings are in line with the observed increase in the number of inhibitory inputs onto the POMC neurons in these mice, as previously it was shown that leptin exerts its effect on POMC neurons, at least in part, by the suppression of their inhibitory inputs[13,14]. The effect of the selective knockout of *LepR* in astrocytes on mIPSCs (but not on mEPSCs) recapitulated the effects of leptin we observed in *Lep$^{ob/ob}$* mice regarding miniature events

on the POMC neurons[11]. On the other hand, while the morphological observations of the current study mimicked the electrophysiological findings regarding IPSCs seen here and in our earlier work[11], the lack of a measurable effect of leptin on mEPSCs of POMC cells was not reflected in morphological alterations regarding putative excitatory inputs. These discrepancies may be due to the fact that leptin signaling is more broadly impacted in *Lep*$^{ob/ob}$ mice, but it also highlights the idea that the interrogation of circuit integrity and function cannot be reliably asserted by a single approach.

Next, we determined the responses of GFAP-LepR$^{-/-}$ mice to fasting or ghrelin, a gut hormone that is elevated during negative energy balance and promotes feeding behavior[15,16]. Fasting-induced hyperphagia was significantly enhanced in these mice compared to controls (Fig 3e,h). They also showed elevated ghrelin-induced food intake (Fig. 3f). Aligned with these findings, AgRP neurons of GFAP-LepR$^{-/-}$ mice exhibited an increased number of Fos expressing nuclei in response to fasting compared to controls (Fig. 3g,h). These observations are consistent with the findings that food deprivation or ghrelin administration elevates AgRP neuronal activity, at least in part, by mediation of presynaptic excitatory inputs, which are now revealed to be controlled by astrocytes.

Collectively, our data show that leptin receptor signaling in astrocytes plays a previously underappreciated active role at the arcuate nucleus interface between afferent hormones, hypothalamic synaptic adaptations and strength and CNS control of feeding. To what extent these processes may be involved in the development of obesity in response to overnutrition and the identity of the intercellular signaling modalities that enables glial cells to alter synaptology need to be determined.

Online Methods

Animal

Two transgenic mice lines *(*GFAP-CreERT2 *and Lepr*$^{flox/flox}$ mice) were obtained and crossed. GFAP-CreERT2 mice[10], which are an inducible transgenic mice under control of human GFAP promoter and estrogen (C57BL/6J background, generated by Flora M. Vaccarino, Yale University School of Medicine, USA) were mated with *Lepr*$^{flox/flox}$ mice[18] (Generated by Streamson Chua, Albert Einstein College of Medicine, USA), and bleeding cages were maintained by mating *Lepr*$^{flox/flox}$ and *Lepr*$^{flox/flox}$:GFAP-CreERT2 mice. To excise loxP sites by Cre recombination, 5-week-old male mice were administrated tamoxifen twice a day (100 mg/kg, i.p.) for five days. Tamoxifen (Sigma-Aldrich) was dissolved in sunflower oil at a final concentration of 10 mg/ml at 37°C, and then filter sterilized and stored for up to 7 days at 4°C in the dark. All control groups are tomoxifen-injected littermate control mice (*Lepr*$^{flox/flox}$). Genotyping was done by PCR using primer sets binding to the *Cre* gene (Cre-1084, 5′-GCG GTC TGG CAG TAA AAA CTA TC-3′; Cre-1085, 5′-GTG AAA CAG CAT TGC TGT CAC TT-3′; Cre-42, 5′-CTA GGC CAC AGA ATT GAA AGA TCT-3′, Cre-43, 5′-GTA GGT GGA AAT TCT AGC ATC ATC C-3′) and crossing the loxP site (65A, 5′-AGA ATG AAA AAG TTG TTT TGG GA-3′; 105, 5′-ACA GGC TTG AGA ACA TGA ACA C-3′; 106, 5′-GTC TGA TTT GAT AGA TGG TCT T-3′). To generate POMC or NPY neuron-specific GFP labeled mice, *Lepr*$^{flox/flox}$:GFAP-CreERT2 mice were mated with transgenic mice expressing GFP in

POMC neurons (#008322, Jackson Laboratories) or hrGFP in NPY neurons (#006417, Jackson Laboratories). To confirm specific *Cre*-mediated recombination in GFAP-positive cell, inducible *Cre* expression was screened by mice line [GFAP-CreERT2 + *Gt(ROSA)26Sor*$^{tm14(CAG-tdTomato)Hze}$ (#007914, Jackson Laboratories)] with injection of tomoxifen (100 mg/kg, i.p.) twice a day for 5 consecutive days. To identify expression of leptin receptor in astrocyte, we used the mouse model[19] (*LepRb-Cre* + Rosa26^{EGFP}; obtained from Martin G. Myers Jr) that expresses enhanced green fluorescent protein (EGFP) in leptin receptor positive cells. All animals were kept in temperature- and humidity-controlled rooms on a 12-h:12-h light:dark cycle, with lights on from 7:00 a.m. to 7:00 p.m. Mice were group housed (3–5 mice per cage) and food and water were provided *ad libitum*. All procedures were approved by the Institutional Animal Care and Use Committee of Yale University.

Food intake measurement

All mice used in these studies were two-month-old male and individually caged five days prior to the start feeding studies to allow the animals to acclimatize to their new environment. For the fasting-induced feeding behavior, 1 and 3 h rebounded food intake were measured after 18 h food deprivation (beginning at 2 h before the dark cycle). For the ghrelin-induced feeding, mice received ghrelin (3 mg/kg of body weight, i.p.) at the early light cycle (ZT 3). Food pellet were weighted and added to the mouse cage 30 min after ghrelin injection and 1h food intake was measured. To determine the leptin response on feeding behavior, mice were food deprived for overnight (18 h) and then received leptin (3 mg/kg of body weight, i.p) 2 h after the dark cycle (ZT 14). 1 and 2 h food intake were measured 30 min after leptin injection. To determine effect of repetitive injection of leptin on daily food intake, food intake was measured every day for 5 days after daily administration of leptin (3 mg/kg of body weight, i.p).

Analysis of metabolic phenotype

Three-month-old male mice were acclimated in metabolic chambers (TSE Systems) for 4 d before the start of the recordings. Mice were continuously recorded for 3 d with the following measurements being taken every 30 min: water intake, food intake, ambulatory activity (in X and Z axes), and gas exchange (O_2 and CO_2) (using the TSE LabMaster system). VO_2, VCO_2, and energy expenditure were calculated according to the manufacturer's guidelines (PhenoMaster Software, TSE Systems). Body composition was measured utilizing MRI (EchoMRI).

Electron microscopy

Under deep anesthesia, three-month-old male mice were perfused (4% paraformaldehyde, 0.1% glutaraldehyde, and 15% picric acid in phosphate buffer), and their brains were processed for immunolabeling for electron microscopy studies. Ultrathin sections were cut on a Leica Ultra-Microtome, collected on Formvar-coated single-slot grids, and analyzed with a Tecnai 12 Biotwin electron microscope (FEI). The electron microscopy photographs (×11,500) were used to measure astrocytic coverage and number of synapses on perikaryal membrane of POMC and unlabeled neurons. The analysis of synapse number was performed

in an unbiased fashion as described elsewhere[3,20]. The analysis of the astrocytic coverage was performed as described previous reports[5,6]. All investigators were blinded to the experimental groups during the entire procedure.

Electrophysiology

GFAP-LepR$^{+/+}$ and GFAP-LepR$^{-/-}$ mice (four-week-old male) labeled with the *Pomc GFP* or *Npy hrGFP* were killed at the beginning of the dark cycle, and the ARC was sliced into 250 μm slices (2/mouse), containing the *Pomc-GFP* or *Npy-hrGFP cells*. Slices were then incubated with artificial CSF (aCSF) at 35 °C for 4 h. After stabilization in aCSF, slices were transferred to the recording chamber for recording mIPSCs and mEPSCs as described previously[3,21].

Immunohistochemistry

Three-month-old male mice were anesthetized and transcardially perfused with 0.9% saline containing heparin (10 mg/L) followed by fixative (4% paraformaldehyde, 15% picric acid, 0.1% glutaraldehyde in 0.1 M PB). Brains were collected and post-fixed overnight before coronal sections were taken at every 50 μm. Sections were washed and then treated with 1% H_2O_2 for 15 min to remove endogenous peroxidase activity. After washing and blocking with 2% normal horse serum, sections were incubated with primary antibodies [anti-mouse GFAP, 1:1000 for 2 h at room temperature (RT), Sigma, G3893; anti-rabbit c-fos, 1:2000 for overnight at RT, Millipore, ABE457; anti-chicken GFP, 1/2000 for overnight at RT, Abcam, ab13970; anti-mouse NeuN, 1/1000 for overnight at RT, Millipore, MAB377; anti-rabbit Iba-1, 1/2000 for overnight at RT, Wako, 019-19741]. The following day, sections were extensively washed and incubated in biotinylated anti-rabbit secondary antibody, ABC reagent, and diaminobenzidine (DAB) substrate (Vector Laboratories). Crystal violet staining was performed to detect cell nuclei. Immunofluorescence was performed with a combination of Alexa Fluor 488–or Alexa Fluor 594–labeled anti-rabbit, anti-chicken, or anti-mouse secondary antibody (1:500 for 1 h at RT, Invitrogen). Representative images were selected from at least 3 times repeated experiments.

Quantification of astrocyte number and projections

For the quantitative evaluation of astrocytes, six sections throughout the arcuate nucleus per animal were analyzed. Astrocytes were detected by DAB-based immunohistochemistry with GFAP antibody followed by crystal violet staining to identify their nuclei. Images were captured with a X40 objective using a digital camera and analyzed using ImageJ software. Cells were counted according to the optical disector technique[3]. The number of primary projections was determined for each GFAP positive cell that was included entirely in the field of analysis and Sholl's analysis[7] was performed to assess differences in the extension of glial processes as described by Del Cerro et al.[22].

Detection of leptin receptor mRNA in astrocyte (In situ hybridization)

To verify animal model in this study with specific deletion of leptin receptor expression in astrocytes, we combined in situ hybridization with immunohistochemistry using astrocyte-specific leptin receptor knock out (GFAP-LepR$^{-/-}$) mice and their control mice (GFAP-

LepR$^{+/+}$). To this end, we designed leptin receptor-specific riboprobes to specifically recognize mRNA region corresponding to *LepR*-delta exon 17 allele (NM_146146 from NCBI gene bank). The riboprobes were labeled with S^{35} and purified with a spin RNA column (Roche Diagnostics). Brain tissues from GFAP-LepR$^{-/-}$ and CT animals were quickly removed, frozen in liquid nitrogen, coronally sectioned at 20 μm thickness using a cryostat, and stored in -80°C until use. First, we performed radioactive in situ hybridization using the S^{35}-labeled riboprobes as above following the protocol reported previously[23]. Briefly, sections were fixed with 3% paraformaldehyde solution, acetylated (2.7 ml of triethanolamine and 0.5 ml of acetic anhydride in 200 ml of RNase-free water), dehydrated through a series of alcohols, and then hybridized with the riboprobes at 52°C for overnight. The next day, the sections were washed through regular washing steps[23], and were ready for immunohistochemistry to visualize astrocyte using a GFAP antibody as a molecular marker for astrocyte. After the washing steps, the sections were incubated with a milk blocking buffer (3% fat-free milk, 0.3% Triton X-100 in 0.1M PB) at RT for 30 min. Then a series of antibody incubations was performed as following: anti-mouse GFAP antibody (1:1000 for 2 h at RT, Sigma), anti-rabbit POMC antibody (1:1000 for overnight at RT, phoenix pharmaceuticals, H-029-30) and Alexa-594 conjugated anti-mouse IgG (1:250 dilution in 0.1M PB, Invitrogen) at RT for 1 h. Regular 0.1M PB washing was performed between antibody incubations. The sections were then finally subjected for emulsion autoradiography, and further microscopy.

Astrocyte primary culture

Mice at postnatal day 3 were sacrificed by decapitation and the hypothalamus was collected in DMEM F12 (Gibco) plus 1% antibiotics-antimycotics (Gibco). The hypothalamus was dissociated and the suspension was centrifugued for 7 min at 1000 rpm. The pellet was resuspended with DMEM F12 plus 10% FBS (Gibco by life technologies) and 1% antibiotics-antimycotics. This media was used to seed and grow cells in 25cm^3 culture treated flasks at 37 °C and 5% CO_2. The media was changed every two days until reach the desired confluence. Once confluence was reached, between day 7 to 9 in vitro, the flasks were place in an incubator shaker at 280 rpm at 37 °C overnight. After shaking, the cells were then washed with PBS (Gibco), trypsinized and resuspended in DMEM F12 plus 10% FBS and 1% antibiotics-antimycotics. The suspension was centrifugued for 5 min at 1150 rpm. After cell counting, the cells were seeded in poly-L-lysine hydrobromide (10 μg/ml Sigma-Aldrich)-coated six well plates at a concentration of 130,000 cells/well. The cells were grown for 24 h in DMEM F12 containing 10% FBS and 1% antibiotics-antimycotics and then treated with 4-Hydroxytamoxifen at a concentration of 1μM or vehicle during 3 consecutive days. Cells were then collected for RNA extraction and PCR analysis.

RT-PCR and Ribosome profiling

RNA was extracted using QIAGEN RNeasy Micro Kit (#74004). cDNA was synthetized using QIAGEN Whole Transcriptome Kit (#207043). RT-PCR was performed in a Roche 480 LightCycler using Taqman probes [*Agrp* (Mm00475829_g1); *Leprb* (Mm01262069_m1); *NeuN* (Mm01248771_m1); *s100β* (Mm00485897_m1)]. To validate the deletion of exon 17 in cording region of the leptin receptor gene, we designed specific primer set (Forward, 5′- TCG ACA AGC AGC AGA ATG AC -3′; Reverse, 5′- CTG CTG

GGA CCA TCT CAT C -3′) and performed RT-PCR with tamoxifen-treated astrocyte primary cells.

Translating Ribosome Affinity Purification (TRAP) was conducted in homogenate samples of hippocampus and hypothalamus obtained from *AldH-EGFP-L10a* mice, which express green fluorescent protein in ribosomes of *AldH*+ cells and *Rpl22* (ribosome protein subunit 22) floxed mice[24] crossed with *Agrp cre* line, which express Rpl22 and HA proteins in ribosomes of AgRP neurons, thus allowing for the immunoprecipitation of polysomes directly from astrocytes and AgRP neurons.[24] TRAP methods were conducted as previously published [25,26,27]. After RNA isolation, we obtained approximately 10 to 25 ng of RNA per sample. RT-PCR was performed as described above.

Statistical analyses

Statistical analyses were performed by use of Prism 6.0 software (Graph Pad, San Diego, CA, USA). Data distribution was assumed to be normal but this was not formally tested. No statistical methods were used to predetermine sample sizes but our sample sizes are similar to those reported in previous publication[16, 28]. All analyses were performed in a blinded manner. No randomization was used to assign experimental groups or to collect data but mice and cells were assigned to specific experimental groups without bias. Unpaired *t*-test was performed to analyze significance between two experimental groups. Two-way ANOVA analysis was performed to detect interaction between treatment and genotype. Two-way repeated measures ANOVA analysis was used to detect interaction between time and genotype. Significance was taken at $p<0.05$.

Supplementary Material

Refer to Web version on PubMed Central for supplementary material.

Acknowledgments

This work was supported by NIH (DP1 DK006850, R01AG040236 and P01NS062686), the American Diabetes Association, the Helmholtz Society (ICEMED) and the Klarmann Family Foundation.

References

1. Belanger M, Allaman I, Magistretti PJ. Brain energy metabolism: focus on astrocyte-neuron metabolic cooperation. Cell metabolism. 2011; 14:724–738. [PubMed: 22152301]
2. Allaman I, Belanger M, Magistretti PJ. Astrocyte-neuron metabolic relationships: for better and for worse. Trends in neurosciences. 2011; 34:76–87. [PubMed: 21236501]
3. West MJ, Gundersen HJ. Unbiased stereological estimation of the number of neurons in the human hippocampus. The Journal of comparative neurology. 1990; 296:1–22. [PubMed: 2358525]
4. Diano S, Naftolin F, Horvath TL. Kainate glutamate receptors (GluR5-7) in the rat arcuate nucleus: relationship to tanycytes, astrocytes, neurons and gonadal steroid receptors. Journal of neuroendocrinology. 1998; 10:239–247. [PubMed: 9630393]
5. Horvath TL, et al. Synaptic input organization of the melanocortin system predicts diet-induced hypothalamic reactive gliosis and obesity. Proceedings of the National Academy of Sciences of the United States of America. 2010; 107:14875–14880. [PubMed: 20679202]
6. Fuente-Martin E, et al. Leptin regulates glutamate and glucose transporters in hypothalamic astrocytes. The Journal of clinical investigation. 2012; 122:3900–3913. [PubMed: 23064363]

7. Sholl DA. A comparative study of the neuronal packing density in the cerebral cortex. Journal of anatomy. 1959; 93:143–158. [PubMed: 13641114]
8. Hsuchou H, Pan W, Barnes MJ, Kastin AJ. Leptin receptor mRNA in rat brain astrocytes. Peptides. 2009; 30:2275–2280. [PubMed: 19747514]
9. Hsuchou H, et al. Obesity induces functional astrocytic leptin receptors in hypothalamus. Brain : a journal of neurology. 2009; 132:889–902. [PubMed: 19293246]
10. Ganat YM, et al. Early postnatal astroglial cells produce multilineage precursors and neural stem cells in vivo. The Journal of neuroscience : the official journal of the Society for Neuroscience. 2006; 26:8609–8621. [PubMed: 16914687]
11. Garcia-Caceres C, et al. Differential acute and chronic effects of leptin on hypothalamic astrocyte morphology and synaptic protein levels. Endocrinology. 2011; 152:1809–1818. [PubMed: 21343257]
12. Gao Q, Horvath TL. Neurobiology of feeding and energy expenditure. Annual review of neuroscience. 2007; 30:367–398.
13. Cowley MA, et al. Leptin activates anorexigenic POMC neurons through a neural network in the arcuate nucleus. Nature. 2001; 411:480–484. [PubMed: 11373681]
14. Vong L, et al. Leptin action on GABAergic neurons prevents obesity and reduces inhibitory tone to POMC neurons. Neuron. 2011; 71:142–154. [PubMed: 21745644]
15. Cowley MA, et al. The distribution and mechanism of action of ghrelin in the CNS demonstrates a novel hypothalamic circuit regulating energy homeostasis. Neuron. 2003; 37:649–661. [PubMed: 12597862]
16. Andrews ZB, et al. UCP2 mediates ghrelin's action on NPY/AgRP neurons by lowering free radicals. Nature. 2008; 454:846–851. [PubMed: 18668043]
17. Yang Y, Atasoy D, Su HH, Sternson SM. Hunger states switch a flip-flop memory circuit via a synaptic AMPK-dependent positive feedback loop. Cell. 2011; 146:992–1003. [PubMed: 21925320]
18. McMinn JE, et al. Neuronal deletion of Lepr elicits diabesity in mice without affecting cold tolerance or fertility. American journal of physiology. Endocrinology and metabolism. 2005; 289:E403–411. [PubMed: 15870101]
19. Patterson CM, Leshan RL, Jones JC, Myers MG Jr. Molecular mapping of mouse brain regions innervated by leptin receptor-expressing cells. Brain research. 2011; 1378:18–28. [PubMed: 21237139]
20. Diano S, et al. Ghrelin controls hippocampal spine synapse density and memory performance. Nature neuroscience. 2006; 9:381–388.
21. Caron E, Sachot C, Prevot V, Bouret SG. Distribution of leptin-sensitive cells in the postnatal and adult mouse brain. The Journal of comparative neurology. 2010; 518:459–476. [PubMed: 20017211]
22. Del Cerro S, Garcia-Estrada J, Garcia-Segura LM. Neuroactive steroids regulate astroglia morphology in hippocampal cultures from adult rats. Glia. 1995; 14:65–71. [PubMed: 7615347]
23. Jeong JK, Chen Z, Tremere LA, Pinaud R. Double fluorescence in situ hybridization in fresh brain sections. Journal of visualized experiments : JoVE. 2010
24. Sanz E, et al. Cell-type-specific isolation of ribosome-associated mRNA from complex tissues. Proceedings of the National Academy of Sciences of the United States of America. 2009; 106:13939–13944. [PubMed: 19666516]
25. Heiman M, et al. A translational profiling approach for the molecular characterization of CNS cell types. Cell. 2008; 135:738–748. [PubMed: 19013281]
26. Doyle JP, et al. Application of a translational profiling approach for the comparative analysis of CNS cell types. Cell. 2008; 135:749–762. [PubMed: 19013282]
27. Dougherty JD, Schmidt EF, Nakajima M, Heintz N. Analytical approaches to RNA profiling data for the identification of genes enriched in specific cells. Nucleic acids research. 2010; 38:4218–4230. [PubMed: 20308160]
28. Dietrich MO, et al. AgRP neurons regulate development of dopamine neuronal plasticity and nonfood-associated behaviors. Nat Neurosci. 2012; 15:1108–1110. [PubMed: 22729177]

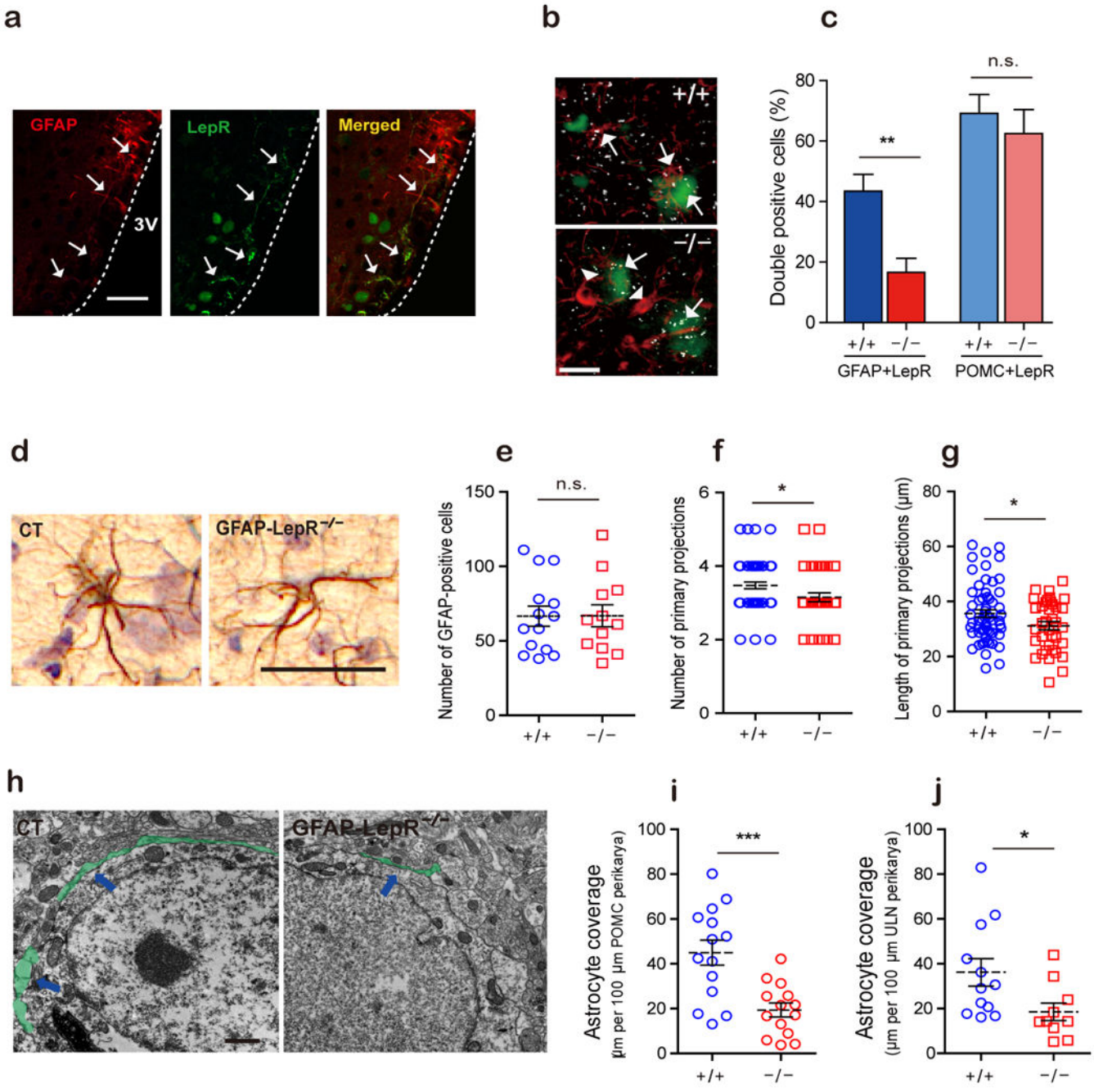

Fig. 1. Cell autonomous impairment of leptin receptor signaling alters astrocyte morphology and reduces astrocytic coverage onto melanocortin cells

(a) Double fluorescence labeling of the astrocyte marker GFAP (red) and leptin receptors (leptin receptor-driven expression of EGFP, green) shows co-localization of GFAP-immunolabeling with EGFP-tagged leptin receptor-containing profiles (white arrows) in the arcuate nucleus (Arc). Scale bar = 100 um. **(b)** The truncated leptin receptor (exon 17) allele was confirmed by *in situ* hybridization combined with immunohistochemistry. Red fluorescence indicates GFAP-positive astrocyte and green fluorescence indicates POMC neurons. White dots indicate mRNA signals of the leptin receptor containing exon 17. **(c)**

Bar graphs show the number of astrocytes or POMC cells expressing mRNA of leptin receptor in the Arc (GFAP+LepR: n=6 slices for GFAP-LepR$^{+/+}$ (+/+); n=6 slices for GFAP-LepR$^{-/-}$ (−/−), p=0.0041, t(10)=3.699; POMC+LepR: n=6 slices for GFAP-LepR$^{+/+}$; n=6 slices for GFAP-LepR$^{-/-}$, p=0.524, t(10)=0.6603). White arrows indicate cells expressing mRNA of leptin receptors. White arrowheads indicate leptin receptor-negative cells. **(d)** Representative image of GFAP-immunolabeling in the Arc of GFAP-LepR$^{+/+}$ and GFAP-LepR$^{-/-}$ mice. Scale bar = 100 μm. **(e)** The number of GFAP-positive cells did not differ between GFAP-LepR$^{+/+}$ and GFAP-LepR$^{-/-}$ mice (n=14 slices for GFAP-LepR$^{+/+}$; n=12 slices for GFAP-LepR$^{-/-}$, p=0.9802, t(24)=0.02503) but (f) the number of primary projections (n=59 cells for GFAP-LepR$^{+/+}$; n=39 cells for GFAP-LepR$^{-/-}$, p=0.0334, t(96)=2.158) and **(g)** their length (n=59 cells for GFAP-LepR$^{+/+}$; n=37 cells for GFAP-LepR$^{-/-}$, p=0.0403, t(94)=2.079) were less in GFAP-LepR$^{-/-}$ mice compared to GFAP-LepR$^{+/+}$ mice. **(h)** Representative electron micrograph showing astrocyte coverage (green pseudo-color and blue arrows) onto POMC-labeled cells. Scale bar = 1 μm. **(i)** POMC cells (n=14 cells or GFAP-LepR$^{+/+}$; n=14 cells or GFAP-LepR$^{-/-}$, p=0.0005, t(26)=3.989) as well as (j) unlabeled neurons (ULN) (n=12 cells for GFAP-LepR$^{+/+}$; n=10 cells for GFAP-LepR$^{-/-}$, p=0.0316, t(20)=1.967) in their vicinity of GFAP-LepR$^{-/-}$ mice had less coverage of their perikaryal membranes by astrocytic processes compared to controls. *, $p<0.05$; **, $p<0.01$; ***, $p<0.001$ *versus* (+/+). Results are means ± the s.e.m. P values for unpaired comparisons were analyzed by two-tailed Student's *t*-test.

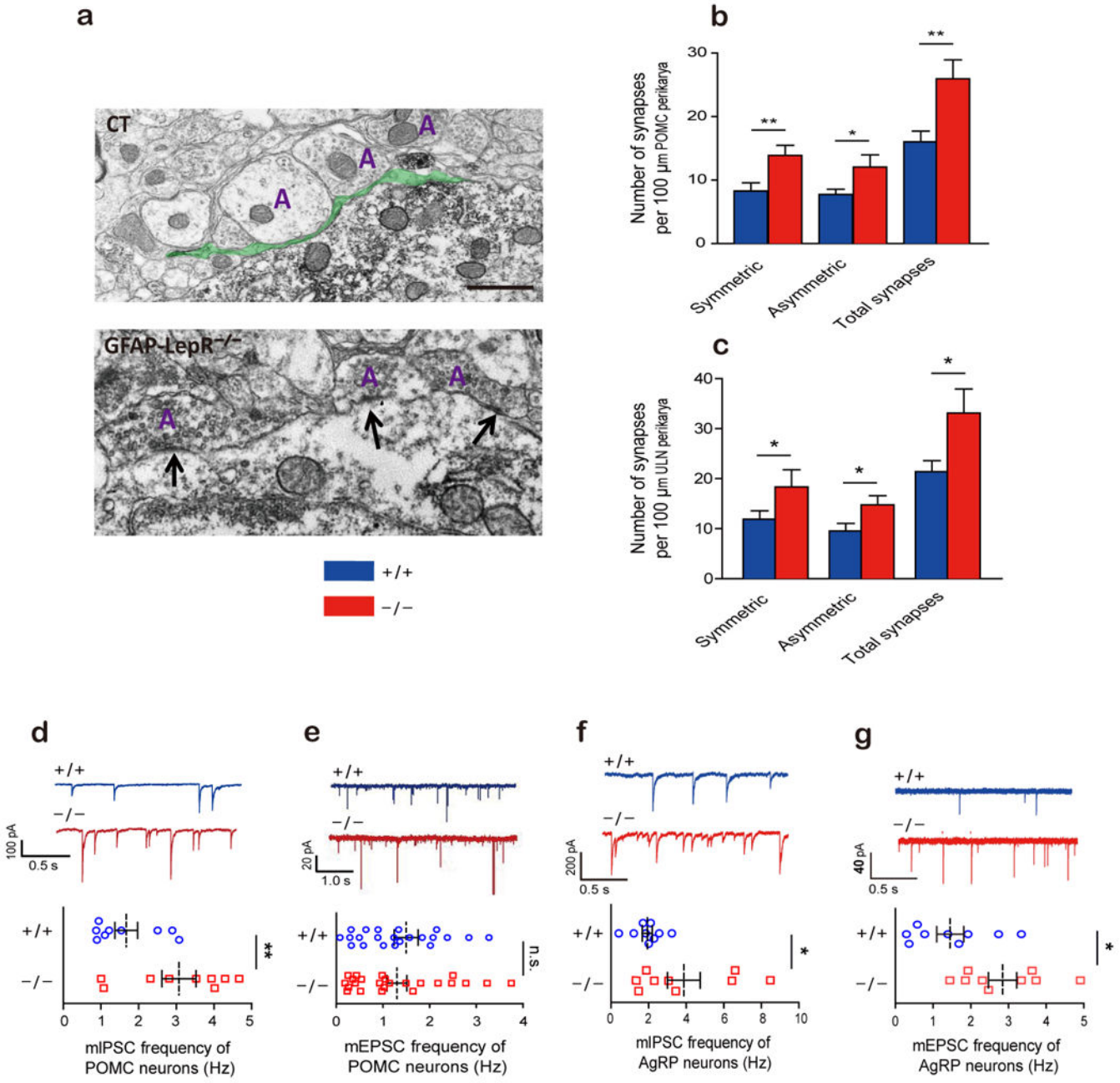

Fig. 2. Impaired leptin receptor signaling in astrocytes increases the number of synapses onto POMC and AgRP neurons

(a) Representative electron micrograph showing astrocyte coverage (green pseudocolor) and synapses (black arrows) onto POMC-labeled cells. Scale bar = 1 µm. **(b)** POMC cells (n=19 cells for GFAP-LepR$^{+/+}$ (+/+); n=15 cells for GFAP-LepR$^{-/-}$ (−/−), p=0.0097, t(32)=2.751 for Symmetric; p=0.0311, t(32)=2.255 for Asymmetric; p=0.0047, t(32)=3.039 for Total) as well as **(c)** unlabeled neurons (ULN) (n=12 cells for GFAP-LepR$^{+/+}$; n=10 cells for GFAP-LepR$^{-/-}$, p=0.0466, t(20)=1.763 for Symmetric; p=0.0352, t(20)=2.259 for Asymmetric; p=0.0297, t(20)=2.341 for Total) in their vicinity of GFAP-LepR$^{-/-}$ mice had elevated numbers of symmetric, asymmetric and hence, total number of synapses on their perikaryal

membrane compared to controls. **(d)** POMC neurons (identified by *POMC-driven GFP* labeling) of GFAP-LepR$^{-/-}$ mice had an elevated frequency of mIPSCs (n=9 cells for GFAP-LepR$^{+/+}$; n=9 cells for GFAP-LepR$^{-/-}$, p=0.0203, t(16)=2.576) but **(e)** no changes in frequency of mEPSCs (n=23 cells for GFAP-LepR$^{+/+}$; n=25 cells for GFAP-LepR$^{-/-}$, p=0.5513, t(45)=0.6003). AgRP neurons (identified by *NPY-driven hrGFP* labeling) of GFAP-LepR$^{-/-}$ mice had an elevated frequency of **(f)** mIPSCs (n=9 cells for GFAP-LepR$^{+/+}$; n=9 cells for GFAP-LepR$^{-/-}$, p=0.0493, t(16)=2.127) and **(g)** mEPSCs (n=9 cells for GFAP-LepR$^{+/+}$; n=9 cells for GFAP-LepR$^{-/-}$, p=0.0164, t(16)=2.681). *, $p<0.05$; **, $p<0.01$ *versus* (+/+). Results are means ± the s.e.m. P values for unpaired comparisons were analyzed by two-tailed Student's *t*-test.

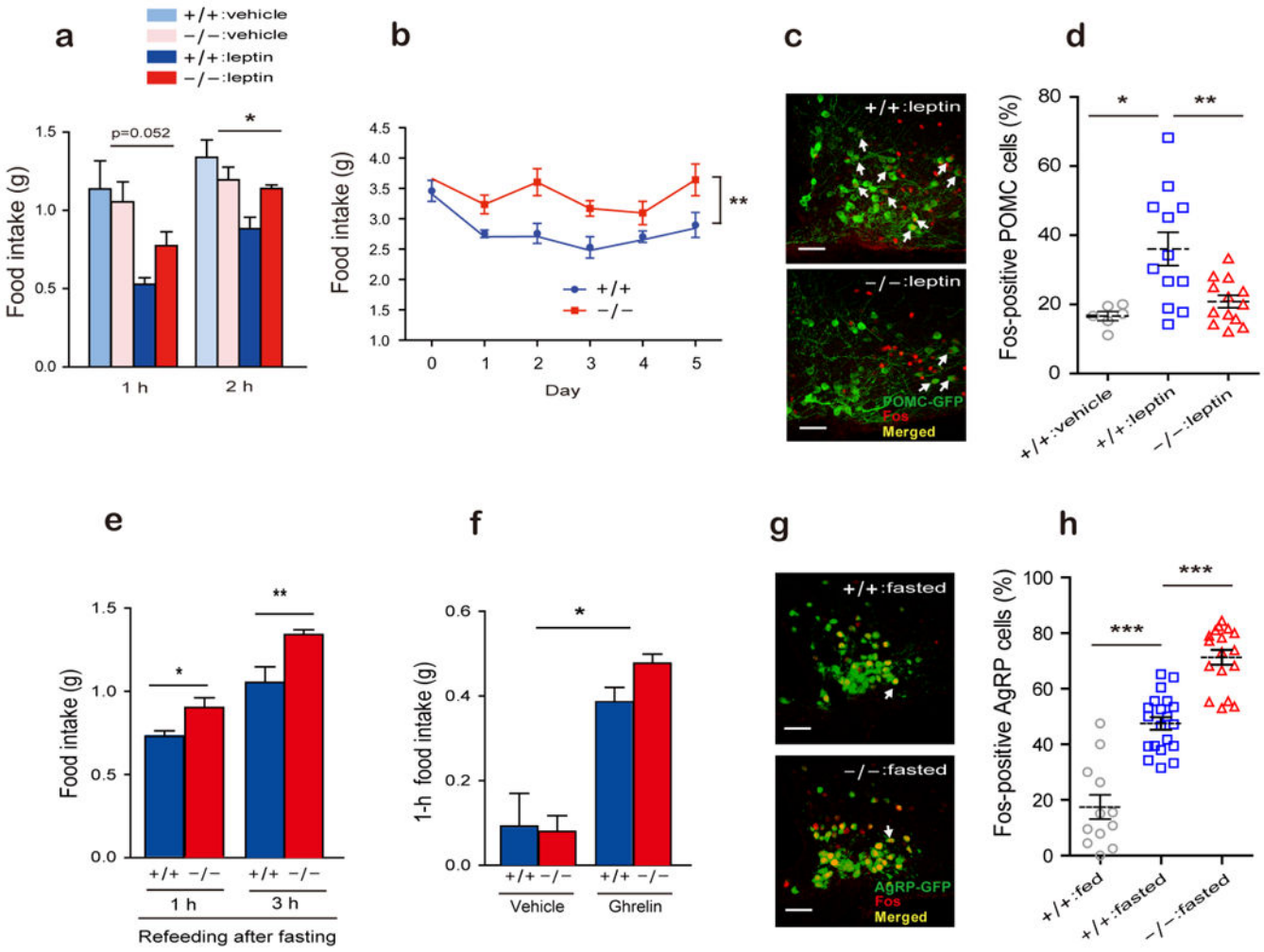

Fig. 3. Impairment of leptin receptor signaling in astrocytes blunts leptin-induced anorexia and enhances fasting or ghrelin-induced hyperphagia

(a, b) GFAP-LepR$^{-/-}$ (−/−) mice showed blunted suppression of feeding in response to leptin administration (Fig. 3a: n=5 mice for GFAP-LepR$^{+/+}$ (+/+)-vehicle, GFAP-LepR$^{-/-}$-vehicle and GFAP-LepR$^{-/-}$-leptin; n=6 mice for GFAP-LepR$^{+/+}$-leptin, p=0.052, F(1,17)=4.386 for 1 h; p=0.018, F(1,17)=6.873 for 2 h; Fig. 3b: n=6 mice per group, p=0.0095, F(9,36)=2.971). **(c)** Representative images show double labeled POMC-GFP and Fos cells in the Arc of GFAP-LepR$^{+/+}$ and GFAP-LepR$^{-/-}$ mice. Scale bar = 100 μm. **(d)** Number of Fos-positive POMC cells induced by leptin treatment was reduced in GFAP-LepR$^{-/-}$ mice (n=6 slices for GFAP-LepR$^{+/+}$-vehicle; n=12 slices for GFAP-LepR$^{+/+}$-leptin; n=13 slices for GFAP-LepR$^{-/-}$-leptin, p=0.013, t(16)=2.788 for GFAP-LepR$^{+/+}$-vehicle versus GFAP-LepR$^{+/+}$-leptin; p=0.0056, t(23)=3.055 for GFAP-LepR$^{+/+}$-leptin versus GFAP-LepR$^{-/-}$-leptin). **(e, f)** GFAP-LepR$^{-/-}$ mice showed increased feeding after fasting or ghrelin administration (Fig 3e: n=6 mice for GFAP-LepR$^{+/+}$; n=7 mice for GFAP-LepR$^{-/-}$, p=0.0378, t(11)=2.361 for 1 h; p=0.0092, t(11)=3.150 for 3 h; Fig 3f: n=5 mice for GFAP-LepR$^{+/+}$-vehicle; n=6 mice for GFAP-LepR$^{-/-}$-vehicle; n=12 mice for GFAP-LepR$^{+/+}$-ghrelin; n=11 mice for GFAP-LepR$^{-/-}$-ghrelin, p=0.04, F(1,32)=4.57). (g) Representative

images show double labeled AgRP-GFP and Fos cells in the Arc of GFAP-LepR$^{+/+}$ and GFAP-LepR$^{-/-}$ mice. Scale bar = 100 μm. (h) Number of Fos-positive AgRP cells induced by overnight fasting was enhanced in GFAP-LepR$^{-/-}$ mice (n=12 slices for GFAP-LepR$^{+/+}$-fed; n=20 slices for GFAP-LepR$^{+/+}$-fasted; n=17 slices for GFAP-LepR$^{-/-}$-fasted, $p<0.0001$, $t(30)=6.721$ for GFAP-LepR$^{+/+}$-fed versus GFAP-LepR$^{+/+}$-fasted; $p<0.0001$, $t(35)=6.848$ for GFAP-LepR$^{+/+}$-fasted versus GFAP-LepR$^{-/-}$-fasted). White arrows indicate double-labeled cells. *, $p<0.05$; **, $p<0.01$; ***, $p<0.001$ versus (+/+), leptin or fasted. Results are means ± the s.e.m. P values for unpaired comparisons were analyzed by two-tailed Student's *t*-test. Two-way ANOVA was performed to detect significant interaction between genotype and treatment (leptin or ghrelin). Two-way repeated measures ANOVA was performed to detect significant interaction between genotype and time (multiple injections of leptin).